Xue *et al. EURASIP Journal on Wireless Communications and Networking* (2017) 2017:31
DOI 10.1186/s13638-017-0820-8

EURASIP Journal on Wireless Communications and Networking

RESEARCH Open Access

An efficient beam-training scheme for the optimally designed subarray structure in mmWave LoS MIMO systems

Chunlin Xue[1], Shiwen He[1,2*], Yongming Huang[1], Yongpeng Wu[3] and Luxi Yang[1]

Abstract

This paper studies the fundamental relations between key design parameters of millimeter wave (mmWave) multiple input multiple output (MIMO) communication systems and subarray structures deployed at both the transmitter and the receiver with each radio frequency (RF) chain connected to only a specific subset of the antennas. The concept of effective degrees of freedom (EDoF) is introduced to measure the maximum spatial multiplexing gain available for the MIMO system. An analytical expression for the EDoF with respect to the parameters of antenna configuration and transmission distance is obtained for the line of sight (LoS) scenario. In addition, the upper and lower bounds of the EDoF are further obtained for some special cases. A fast beam training algorithm based on the codebook is developed to reduce the number of training for the designed mmWave system. Extensive simulation results indicate that the proposed scheme reduces the computational load of the exhaustive approach with only minimal loss in performance. Moreover, the proposed design is robust to the geometrical change and misplacement.

Keywords: Millimeter wave (mmWave), Antenna deployment, Beam training, Line of sight (LoS), Multiple input multiple output (MIMO)

1 Introduction

Motivated by the ever increasing growth in multimedia applications and the number of users, millimeter wave (mmWave) has been regarded as an essential technique for the next generation wireless communication network [1]. The multiple gigabit per second (Gbps) date rate requirements of future broadband systems can be satisfied by large swathes of unlicensed spectrums around the mmWave band [2]. Besides, the remarkable advancements in the mmWave hardware make it feasible to adopt mmWave band in many applications [3]. Spectral efficiencies can be further improved by employing multiple antennas, where multiple independent data streams are transmitted and received in parallel through spatial multiplexing without extra bandwidth or transmit power [4].

The advantages of multiple input multiple output (MIMO) techniques rely heavily on the unique propagation characteristics of wireless channels. It is well known that mmWave channels are usually characterized with sparse scattering structures, which are unfavorable for MIMO systems [5, 6]. Most previous research on MIMO techniques are based on the dense scattering environment to enable spatial multiplexing [4]. While mmWave communications usually take place in the strong line of sight (LoS) circumstances where the channel responses are rank deficient, the spatial multiplexing gain can still be obtained by employing carefully designed antenna arrays thanks to the short wavelength [7]. Some efforts have been made on this topic, both for indoor scenarios [8, 9] and outdoor scenarios [10].

On the other hand, the propagation of mmWave suffers from large path loss due to the small wavelength, which causes the sharp attenuation of signal power and results in disabilities for long distance communications [11, 12]. For outdoor applications, the beamforming technique is regarded as a good solution to compensate the path loss by narrow beams with high array gains

*Correspondence: shiwenhe@seu.edu.cn
[1]School of Information Science and Engineering, Southeast University, Nanjing 210096, China
[2]The Key Laboratory of Cognitive Radio and Information Processing, Ministry of Education, Guilin University of Electronic Technology, Guilin 541004, China
Full list of author information is available at the end of the article

[13, 14]. Digital beamforming is traditionally designed based on channel state information (CSI) to improve communication quality at the advantages of digital processing techniques, such as interference cancellation and formation of multiple simultaneous beams. Analog beamforming is put forward to overcome the radio frequency (RF) hardware limitations where a network of analog phase shifters is employed to control the phase of the signal at each antenna. Due to the high power consumption of the digital scheme [15, 16] and the possible performance loss of the analog scheme, the hybrid beamforming scheme has been presented in [17, 18] to divide the beamforming operations between the analog and digital domains, where the required number of RF chains is reduced. In [19], beam training algorithms are proposed to design the partially-connected subarray antenna structure, which uses a separate RF chain and analog-to-digital converter (ADC) for each phase shifters network. More recently, [20] and [21] have investigated the beamforming codebook design for millimeter systems and demonstrated its superiority over the exhaustive searching protocol. However, the existing investigations have mainly considered beamforming techniques and the optimal design for antennas placement separately. As a result, the balance between spatial multiplexing gains and array gains may be ignored in mmWave communications.

In this paper, we propose an efficient beam-training scheme for mmWave LoS MIMO communication systems with subarray structures at both the transmitter and the receiver. The subarray structure with directional antenna elements and phase shifters is designed to maximize effective degrees of freedom (EDoF) so that more multiplexing gain is available. An estimation for the separation between subarrays is also performed when the required EDoF are smaller than the number of RF chains. The codebook design method from [20] and [21] is employed in the proposed beam training scheme to apply for the situation where explicit CSI is unavailable. Furthermore, the proposed scheme focuses on the selection strategy of codewords and is aimed at shortening training time as much as possible. In a word, the proposed beam training scheme includes several iterative training steps, where codewords from the codebook are selected and trained at each step. Numerical results show that the proposed scheme has some advantages over the existing counterparts.

The rest of this paper is organized as follows. Section 2 introduces the system architecture and channel models, Section 3 provides the optimal design criterion of the normalized subarray separation product for maximizing EDoF in the subarray structure. Section 4 provides the proposed low complexity beam training scheme. Simulation results of EDoF and capacity performance are presented in Section 5, and conclusions are given in Section 6.

Notation: $\mathbf{A}$ is a matrix, $\mathbf{a}$ is a vector, a is a scalar, $(\cdot)^T$ and $(\cdot)^H$ denote transpose and Hermitian conjugate transpose, respectively. $\mathbf{I}_N$ is the $N \times N$ identity matrix, $\mathbf{1}_N$ is the $N \times N$ all-ones matrix, $|\cdot|$ denotes the determinant operation, $\|\cdot\|_F$ denotes the Frobenius norm operation, $\lfloor a \rfloor$ is the largest integer that is smaller than or equal to a, $\lceil a \rceil$ is the smallest integer that is larger than or equal to a, diag $(\mathbf{a})$ is a matrix whose diagonal elements are formed by $\mathbf{a}$, $\mathcal{CN}(\mathbf{a}, \mathbf{A})$ is a complex Gaussian vector with mean $\mathbf{a}$ and covariance matrix $\mathbf{A}$.

2 System model

Considering a point-to-point mmWave MIMO communication system in Fig. 1, where both the transmitter (Tx) and the receiver (Rx) adopt a subarray structure with some phase shifters to construct directional beams. In the subarray structure, each RF chain is connected to only a subset of the antennas, which is different from the fully-connected structure where each RF chain is connected to all antennas. There are totally N_t transmit antennas and N_r receive antennas which are divided into N transmit subarrays and M receive subarrays equally. Without loss of generality, we assume that $M \geqslant N$, and each transmit subarray is equipped with P antennas and each receive subarray is equipped with Q antennas. The antenna elements in each subarray are driven by the same RF chain but connected to a single phase shifter. Then, the complex input-output relationship for this system can be represented mathematically by

$$\mathbf{y} = \mathbf{W}^H\mathbf{H}\mathbf{F}\mathbf{x} + \mathbf{W}^H\mathbf{n} = \widetilde{\mathbf{H}}\mathbf{x} + \widetilde{\mathbf{n}} \tag{1}$$

where $\mathbf{y} \in \mathbb{C}^{M\times 1}$, $\mathbf{H} \in \mathbb{C}^{N_r\times N_t}$, and $\mathbf{x} \in \mathbb{C}^{N\times 1}$ denote the received signal vector, the channel response matrix, and the transmitted signal vector, respectively. $\mathbf{F} = diag\,(\mathbf{f}_0, \mathbf{f}_1, \cdots, \mathbf{f}_{N-1}) \in \mathbb{C}^{N_t\times N}$ is the RF precode matrix, $\mathbf{f}_n$ denotes the beamforming vector for the nth transmit subarray, $\mathbf{W} = diag\,(\mathbf{w}_0, \mathbf{w}_1, \cdots, \mathbf{w}_{M-1}) \in \mathbb{C}^{N_r\times M}$ is the

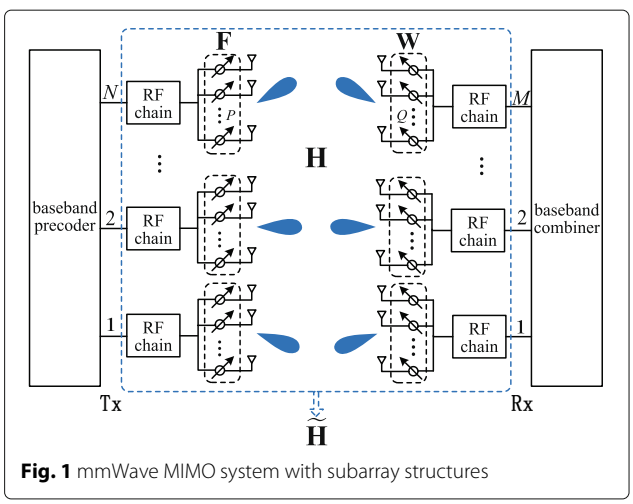

Fig. 1 mmWave MIMO system with subarray structures

RF combine matrix, and $\mathbf{w}_m$ denotes the combining vector for the mth receive subarray. $\widetilde{\mathbf{H}} = \mathbf{W}^H\mathbf{H}\mathbf{F}$ denotes the RF equivalent channel. $\mathbf{n} \in \mathbb{C}^{N_r \times 1}$ is the additive white Gaussian noise (AWGN) vector with distribution $\mathcal{CN}\left(\mathbf{0}, \sigma_n^2\mathbf{I}_{N_r}\right)$, and $\widetilde{\mathbf{n}} = \mathbf{W}^H\mathbf{n}$ denotes the RF equivalent noise vector. The capacity of such a system is given by

$$V = \log_2\left(\left|\mathbf{I}_M + \frac{\rho}{N}\left(\mathbf{W}^H\mathbf{W}\right)^{-1}\widetilde{\mathbf{H}}\widetilde{\mathbf{H}}^H\right|\right) \tag{2}$$

where ρ denotes the average received signal to noise ratio (SNR) at the input of the receiver.

In this paper, the MIMO channel model is expressed as [22]

$$\mathbf{H} = \sqrt{\frac{K_f}{1+K_f}}\mathbf{H}_{\mathrm{LOS}} + \sqrt{\frac{1}{1+K_f}}\mathbf{H}_{\mathrm{NLOS}} \tag{3}$$

where $\mathbf{H}_{\mathrm{LoS}}$ and $\mathbf{H}_{\mathrm{NLoS}}$ denote the LoS component and the non line of sight (NLoS) component, respectively. K_f denotes the ratio between the power of these two components. In general, mmWave channel $\mathbf{H}$ is mainly determined by the LoS component due to the limited number of scatters in the mmWave propagation environment [23, 24]. Therefore, in this paper, we focus on the case where $K_f \to +\infty$.

Considering the antennas layout in Fig. 2, the antenna elements in transmit and receive subarrays are separated by d_t and d_r, respectively. The distance between the last element of one subarray and the first element of the next one subarray is D_t (D_r) for the transmitter (receiver). z_0 is the position shift of the receiver along the z-axis. θ and ϕ are the angles of the local spherical coordinate system at the receiver. Assume that the distance R between the transmitter and the receiver is much larger than d_t, d_r, $S_t = (P-1)\,d_t + D_t$, and $S_r = (Q-1)\,d_r + D_r$. Thus, the effect of path loss differences among antennas can be ignored, and only the phase difference caused by separate propagation paths is considered. In a pure LoS channel, the complex channel gain $h_{s,k}$, representing the (s,k)th element of $\mathbf{H}$, can be modeled as

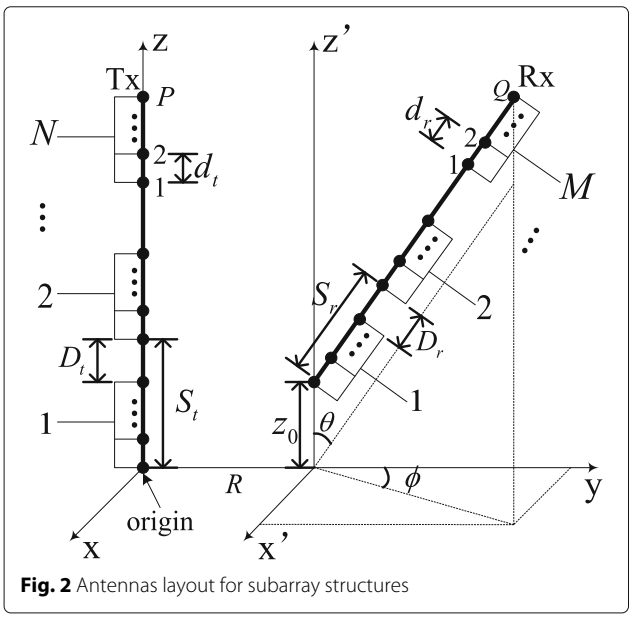

Fig. 2 Antennas layout for subarray structures

$$h_{s,k} = \exp\left(j\frac{2\pi}{\lambda}r_{s,k}\right) \tag{4}$$

where $s = 0, 1, \cdots, N_r - 1$, $k = 0, 1, \cdots, N_t - 1$, λ is the carrier wavelength and $r_{s,k}$ is the distance between the kth transmit antenna and the sth receive antenna. Let $k = nP + p$ and $s = mQ + q$, i.e., the kth transmit antenna is the pth element of the nth transmit subarray and the sth receive antenna is the qth element of the mth receive subarray. Assume that each subarray is the uniform linear array (ULA), then $r_{s,k}$ can be calculated as follows:

$$r_{mQ+q,nP+p} \approx r_{mQ,nP} + pd_t\sin\psi_n + qd_r\sin\gamma_m \tag{5}$$

where $m = 0, 1, \cdots, M-1$, $q = 0, 1, \cdots, Q-1$, $n = 0, 1, \cdots, N-1$, and $p = 0, 1, \cdots, P-1$. ψ_n and γ_m denote the angles of the LoS path from the antenna boresight in the nth Tx subarray and that from the antenna boresight in the mth Rx subarray, respectively. With the knowledge of the geometry, $r_{mQ,nP}$ can be further written as:

$$\begin{aligned} r_{mQ,nP} &= \Big[(R + mS_r\sin\theta\cos\phi)^2 + (mS_r\sin\theta\sin\phi)^2 \\ &\quad + (z_0 + mS_r\cos\theta - nS_t)^2\Big]^{1/2} \\ &\approx R + mS_r\sin\theta\cos\phi \\ &\quad + \frac{(mS_r\sin\theta)^2 + (z_0 + mS_r\cos\theta - nS_t)^2}{2R} \end{aligned} \tag{6}$$

The approximation is obtained via $(1+\Delta)^{1/2} \approx 1 + \frac{\Delta}{2}$ on the condition that $\Delta \ll 1$.

For simplicity, the channel matrix is rewritten as

$$\begin{aligned} \mathbf{H} &= \left[\mathbf{h}_0, \mathbf{h}_1, \cdots, \mathbf{h}_{N_t-1}\right] \\ &= \begin{bmatrix} \mathbf{H}_{0,0} & \mathbf{H}_{0,1} & \cdots & \mathbf{H}_{0,N-1} \\ \mathbf{H}_{1,0} & \mathbf{H}_{1,1} & \cdots & \mathbf{H}_{1,N-1} \\ \vdots & \vdots & \ddots & \vdots \\ \mathbf{H}_{M-1,0} & \mathbf{H}_{M-1,1} & \cdots & \mathbf{H}_{M-1,N-1} \end{bmatrix} \end{aligned} \tag{7}$$

where $\mathbf{h}_k = \left[\exp\left(\frac{j2\pi}{\lambda}r_{0,k}\right), \exp\left(\frac{j2\pi}{\lambda}r_{1,k}\right), \cdots, \exp\left(\frac{j2\pi}{\lambda}r_{N_r-1,k}\right)\right]^T$, and the submatrix $\mathbf{H}_{m,n}$ denotes the channel response from the nth transmit subarray to the mth receive subarray,

$$\mathbf{H}_{m,n} = \begin{bmatrix} h_{mQ,nP} & h_{mQ,nP+1} & \cdots & h_{mQ,nP+P-1} \\ h_{mQ+1,nP} & h_{mQ+1,nP+1} & \cdots & h_{mQ+1,nP+P-1} \\ \vdots & \vdots & \ddots & \vdots \\ h_{mQ+Q-1,nP} & h_{mQ+Q-1,nP+1} & \cdots & h_{mQ+Q-1,nP+P-1} \end{bmatrix}. \tag{8}$$

The RF equivalent channel takes the impact of phase shifters into consideration and reflects the response between each RF chain pair of the transmitter and the receiver

$$\widetilde{\mathbf{H}} = \mathbf{W}^H\mathbf{H}\mathbf{F} = \begin{bmatrix} \mathbf{w}_0^H\mathbf{H}_{0,0}\mathbf{f}_0 & \mathbf{w}_0^H\mathbf{H}_{0,1}\mathbf{f}_1 & \cdots & \mathbf{w}_0^H\mathbf{H}_{0,N-1}\mathbf{f}_{N-1} \\ \mathbf{w}_1^H\mathbf{H}_{1,0}\mathbf{f}_0 & \mathbf{w}_1^H\mathbf{H}_{1,1}\mathbf{f}_1 & \cdots & \mathbf{w}_1^H\mathbf{H}_{1,N-1}\mathbf{f}_{N-1} \\ \vdots & \vdots & \ddots & \vdots \\ \mathbf{w}_{M-1}^H\mathbf{H}_{M-1,0}\mathbf{f}_0 & \mathbf{w}_{M-1}^H\mathbf{H}_{M-1,1}\mathbf{f}_1 & \cdots & \mathbf{w}_{M-1}^H\mathbf{H}_{M-1,N-1}\mathbf{f}_{N-1} \end{bmatrix}. \tag{9}$$

Due to the large size of the antenna array and the large propagation loss, a large number of training data and feedback information is essential to realize the exact phase shifts and amplitude adjustments for the phase shift networks. However, the heavy training overhead is incompatible with the low power consumption and low complexity requirements for mmWave communications [16]. Therefore, a codebook-based solution with only quantized phase shift but without any amplitude adjustment of the elements of the RF precoder is adopted to simplify this procedure and reach a tradeoff between the complexity and the performance. In this paper, the beamformimg vectors and the combining vectors are selected from predefined codebooks, which specify a certain beam direction. Let $\mathbf{C}^t = \left[\mathbf{c}_1^t, \mathbf{c}_2^t, \cdots, \mathbf{c}_{L_t}^t\right]$ $\left(\mathbf{C}^r = \left[\mathbf{c}_1^r, \mathbf{c}_2^r, \cdots, \mathbf{c}_{L_r}^r\right]\right)$ represent the transmit(receive) codebook with size $P \times L_t$ ($Q \times L_r$). Each column of $\mathbf{C}^t$ and $\mathbf{C}^r$ represents a unique beam vector and is given by [20, 21]

$$\mathbf{c}_{l^t}^t = \frac{1}{\sqrt{P}}\left[1, e^{-j\frac{2\pi}{\lambda}d_t\left(1-\frac{2l^t}{L_t}\right)}, \cdots, e^{-j\frac{2\pi}{\lambda}(P-1)d_t\left(1-\frac{2l^t}{L_t}\right)}\right]^T \tag{10}$$

$$\mathbf{c}_{l^r}^r = \frac{1}{\sqrt{Q}}\left[1, e^{-j\frac{2\pi}{\lambda}d_r\left(1-\frac{2l^r}{L_r}\right)}, \cdots, e^{-j\frac{2\pi}{\lambda}(Q-1)d_r\left(1-\frac{2l^r}{L_r}\right)}\right]^T \tag{11}$$

where $l^t = 1, 2, \cdots, L_t$, $l^r = 1, 2, \cdots, L_r$. L_t (L_r) denotes the number of codewords in the transmit(receive) codebook. Thus, (2) is equivalent to

$$V = \sum_{i=1}^{N} \log_2\left(1 + \frac{\rho}{N}\omega_i\right) \tag{12}$$

where ω_i is the ith eigenvalue of $\widetilde{\mathbf{Q}} = \widetilde{\mathbf{H}}^H\widetilde{\mathbf{H}}$.

3 Subarray structure design for LoS MIMO

3.1 Maximum EDoF criterion

It is easy to see that the RF equivalent channel with N transmit RF chains and M receive RF chains can be decomposed into an equivalent system consisting of $\min(N, M)$ parallel SISO subchannels whose channel power gains are the eigenvalues of $\widetilde{\mathbf{Q}}$. The EDoF quantifying the number of the effective SISO subchannels [4] is calculated as

$$EDOF = \frac{d}{d\delta}V\left(2^\delta\rho\right)\Big|_{\delta=0} = \sum_{i=1}^{N}\frac{\rho\omega_i}{N+\rho\omega_i}. \tag{13}$$

(13) shows that the EDoF is a simple function of the average SNR, the number of transmit RF chains, and the eigenvalues of the $\widetilde{\mathbf{Q}}$ matrix. When the average SNR and the eigenvalues are large ($\rho\omega_i \gg N$), a 3 dB increase in SNR gives approximately a capacity increase of 1 bit/s/Hz for each subchannel.

Though the RF equivalent channel matrix $\widetilde{\mathbf{H}}$ has rank $\min(N, M)$ with probability one in general. If the correlation among the components of $\widetilde{\mathbf{H}}$ increases, the gap between the greatest and smallest eigenvalue will becomes lager. As a result, those SISO subchannels with small power gains make little contributions to the channel capacity and become noneffective. Therefore, EDoF can be increased by reducing the correlation between RF chains. Ideally, it is expected that $\left[\widetilde{\mathbf{H}}^H\widetilde{\mathbf{H}}\right]_{n_1,n_2} = 0$ when $n_1 \neq n_2$, i.e.,

$$\left[\widetilde{\mathbf{H}}^H\widetilde{\mathbf{H}}\right]_{n_1,n_2} = \sum_{m=0}^{M-1}\mathbf{f}_{n_1}^H\mathbf{H}_{m,n_1}^H\mathbf{w}_m\mathbf{w}_m^H\mathbf{H}_{m,n_2}\mathbf{f}_{n_2} = 0. \tag{14}$$

Assume that the l_n^tth codeword of the transmit codebook $\mathbf{C}^t$ and the l_m^rth codeword of the receive codebook $\mathbf{C}^r$ are chosen as the beamforming vector for the nth transmit subarray and the combining vector for the mth receive subarray[1], i.e.,

$$\mathbf{f}_n(p) = \frac{1}{\sqrt{P}}e^{-j\frac{2\pi}{\lambda}pd_t\left(1-\frac{2l_n^t}{L_t}\right)} = \frac{1}{\sqrt{P}}e^{-j\frac{2\pi}{\lambda}pd_t\sin\alpha_n} \tag{15}$$

$$\mathbf{w}_m(q) = \frac{1}{\sqrt{Q}}e^{-j\frac{2\pi}{\lambda}qd_r\left(1-\frac{2l_m^r}{L_r}\right)} = \frac{1}{\sqrt{Q}}e^{-j\frac{2\pi}{\lambda}qd_r\sin\beta_m} \tag{16}$$

where $l_n^t \in \{1, 2, \cdots, L_t\}$, $l_m^r \in \{1, 2, \cdots, L_r\}$, $\sin\alpha_n = 1 - \frac{2l_n^t}{L_t}$ and $\sin\beta_m = 1 - \frac{2l_m^r}{L_r}$. Ideally, the beam training scheme can get the result $\alpha_n \approx \psi_n$ and $\beta_m \approx \gamma_m + \pi$ when L_t and

L_r are large enough. Substituting (4), (5), (15) and (16) into (14), we obtain

$$\begin{aligned}&\sum_{m=0}^{M-1}\exp\left(j\frac{2\pi}{\lambda}\left(r_{mQ,n_2P}-r_{mQ,n_1P}\right)\right)\\&=\exp\left(j\frac{\pi}{\lambda R}\left(\left(n_2S_t\right)^2-\left(n_1S_t\right)^2-2z_0\left(n_2-n_1\right)S_t\right)\right)\cdot\\&\sum_{m=0}^{M-1}\exp\left(-j\frac{2\pi m\left(n_2-n_1\right)S_tS_r\cos\theta}{\lambda R}\right)=0\end{aligned}$$

$$\Rightarrow\frac{\sin\left(\frac{\pi}{\lambda R}M\left(n_2-n_1\right)S_tS_r\cos\theta\right)}{\sin\left(\frac{\pi}{\lambda R}\left(n_2-n_1\right)S_tS_r\cos\theta\right)}=0. \quad (17)$$

According to (17), we have $\sin(\frac{\pi}{\lambda R}M\left(n_2-n_1\right)S_tS_r\cos\theta)=0 and \sin\left(\frac{\pi}{\lambda R}\left(n_2-n_1\right)S_tS_r\cos\theta\right)\neq 0$. That is $\frac{\pi}{\lambda R}M\left(n_2-n_1\right)S_tS_r\cos\theta=T_1\pi$ and $\frac{\pi}{\lambda R}\left(n_2-n_1\right)S_tS_r\cos\theta\neq T_2\pi$, where $T_1,T_2\in\mathbb{Z}$, $(n_2-n_1)\in\{1,2,\cdots,N-1\}$. We choose the smallest one from them with $\frac{\pi}{\lambda R}MS_tS_r\cos\theta=\pi$, which corresponds to the smallest separation and is of most interest from the point of practical applications. Then, it can be derived that $\frac{S_tS_r}{\lambda R}=\frac{1}{M\cos\theta}$. Similarly, for $M<N$, we can obtain the similar conclusions. Thus, the generalized result can be expressed as

$$\frac{S_tS_r}{\lambda R}=\frac{1}{\max\{M,N\}\cos\theta}. \quad (18)$$

It is easy to see that the key design parameter of the LoS MIMO communication system with subarray structures is the ratio between the product S_tS_r and λR. For description convenience, we define the normalized subarray separation product as $N_{ssp}=\frac{S_tS_r}{\lambda R}$. When (18) is satisfied, the EDoF of the RF equivalent channel approach the smaller number of RF chains between the transmitter and the receiver and there are $\min(N,M)$ data streams that can be transmitted in parallel effectively. The maximum EDoF criterion is expressed as the relationship among the subarray separation, transmission distance, wavelength and the number of RF chains. It is worth noting that the optimal normalized subarray separation product N_{ssp} is independent of the angle ϕ and the position shift z_0 in Fig. 2. Thus, the optimal separations can be easily determined only if the information about the transmission distance, the carrier frequency and the number of RF chains are known to the transmitter and the receiver. It is worth pointing out that the criterion written as a function of the product of the subarray separations allows a tradeoff between the antenna array sizes of the transmitter and the receiver. If one end of the link is restricted to a certain area, it can be compensated by deploying a larger antenna array at the other end to avoid performance loss of the system. This is a common situation in distributed MIMO applications.

3.2 An estimation of subarray separations for required EDoF

In practice, each data stream can be assigned for more than one RF chains at the advantage of diversity techniques. So the required EDoF is usually smaller than the number of RF chains and Eq. (18) is a stricter condition for the actual system. A looser condition can be derived by determining the dynamic range of the EDoF for a specific antennas deployment.

Equation 13 shows that the EDoF is related to the distribution of eigenvalues of the matrix $\widetilde{\mathbf{Q}}$ besides the average SNR. Using the knowledge of the matrix theory, we can calculate the sum of these eigenvalues as follows

$$\begin{aligned}\sum_{i=1}^{N}\omega_i=tr\left(\widetilde{\mathbf{H}}^H\widetilde{\mathbf{H}}\right)=\left\|\widetilde{\mathbf{H}}\right\|_F^2=\sum_{m=0}^{M-1}\sum_{n=0}^{N-1}\left\|\mathbf{w}_m^H\mathbf{H}_{m,n}\mathbf{f}_n\right\|_F^2\\\leqslant\sum_{m=0}^{M-1}\sum_{n=0}^{N-1}\left\|\mathbf{w}_m^H\right\|_F^2\left\|\mathbf{H}_{m,n}\right\|_F^2\left\|\mathbf{f}_n\right\|_F^2=NMPQ.\end{aligned} \quad (19)$$

When the vector $\mathbf{f}_n$ is linearly dependent on every row of the channel submatrix $\mathbf{H}_{m,n}$ and the vector $\mathbf{w}_m$ is linearly dependent on every column of the channel submatrix $\mathbf{H}_{m,n}$, the equality in (19) is achieved.

It is trivial to show that the minimum EDoF is obtained for $\widetilde{\mathbf{H}}^H\widetilde{\mathbf{H}}=MPQ\mathbf{1}_N$ and $N_{ssp}=0$. This corresponds to an entirely correlated (rank one) RF equivalent channel, and the associated EDoF is equivalent to that of a SISO channel as follows

$$EDOF_{\min}=\frac{\rho\omega_1}{N+\rho\omega_1}=\frac{\rho NMPQ}{N+\rho NMPQ}. \quad (20)$$

Under the other extreme situation, the EDoF in (13) is maximized for $\widetilde{\mathbf{H}}^H\widetilde{\mathbf{H}}=MPQ\mathbf{I}_N$ when the condition (18) holds. This corresponds to a system with perfectly orthogonal RF equivalent subchannels, and the EDoF is then equivalent to that of N independent SISO subchannels as follows

$$EDOF_{\max}=\sum_{i=1}^{N}\frac{\rho\omega_i}{N+\rho\omega_i}<\frac{\rho NMPQ}{N+\rho MPQ}. \quad (21)$$

We use a linear function to estimate the EDoF approximately when $N_{ssp}\in\left[0,\frac{1}{M\cos\theta}\right]$, which is true on condition that the number of subarrays and the number of antennas in each subarray are large enough. If the number of data streams is smaller than the number of RF chains, then the required EDoF can be set smaller than the maximum EDoF. Thus, we can estimate the minimum required normalized subarray separation product $\widehat{N}_{ssp}$ for the required EDoF

$$\widehat{N}_{ssp}=\frac{EDoF_r-EDoF_{\min}}{M\cos\theta\left(EDoF_{\max}-EDoF_{\min}\right)} \quad (22)$$

where $EDoF_r$ denotes the required EDoF.

4 Proposed beam-training scheme

In this section, an efficient beam training scheme is designed for a specific antenna subarray structure where the transmitter and the receiver have the same number of subarrays, i.e., $M = N$.

Due to the difficulty in acquiring CSI for both the transmitter and the receiver in mmWave MIMO systems, we introduce the codebook-based beam training criteria in absence of the channel knowledge. The Tx beamforming vectors and Rx combining vectors are chosen to maximize the beamforming gain as

$$\left(\widehat{\mathbf{f}}_n, \widehat{\mathbf{w}}_n\right) = \max_{\mathbf{f}_n \in \mathbf{C}^t, \mathbf{w}_n \in \mathbf{C}^r} \left\| \mathbf{w}_n^H \mathbf{H}_{n,n} \mathbf{f}_n \right\|_F^2 \tag{23}$$

where $n = 0, 1, \cdots, N-1$. As shown in Fig. 3, the proposed scheme includes the transmit beam training and receive beam training based on the beamforming gain criterion.

The transmit beam training procedure determines the beamforming vectors at the transmitter. Assume that the omnidirectional receiving strategy is adopted in this procedure, so the vector $\mathbf{w}_n$ is removed from (23), e.g.,

$$\widehat{\mathbf{f}}_n = \max_{\mathbf{f}_n \in \mathbf{C}^t} \left\| \mathbf{H}_{n,n} \mathbf{f}_n \right\|_F^2. \tag{24}$$

The transmit beam training procedure is initialized by selecting an original referenced codeword $\mathbf{c}_{l_0}^t$ from the predefined codebook $\mathbf{C}^t$ randomly, where $l_0 \in \{1, 2, \cdots, L_t\}$. The optimal beamforming gain is set as $\zeta_*^t = 0$ at present. For the jth step, a sub-codebook $\mathbf{E}_j^t = \left[\mathbf{e}_1^t, \mathbf{e}_2^t, \cdots, \mathbf{e}_{B_j^t}^t\right]$ is generated as follow, if $j = 1$,

$$\mathbf{e}_i^t = \mathbf{c}^t_{\mathrm{mod}\left(l_{j-1} + i\Delta_j^t, L_t\right)}, i = 1, 2, \cdots, B_j^t \tag{25}$$

else

$$\mathbf{e}_i^t = \begin{cases} \mathbf{c}^t_{\mathrm{mod}\left(l_{j-1} - i\Delta_j^t, L_t\right)} & i = 1, 2, \cdots, \left\lfloor \frac{B_j^t}{2} \right\rfloor \\ \mathbf{c}^t_{\mathrm{mod}\left(l_{j-1} + \left(i - \left\lfloor \frac{B_j^t}{2} \right\rfloor\right)\Delta_j^t, L_t\right)} & i = \left\lfloor \frac{B_j^t}{2} \right\rfloor + 1, \cdots, B_j^t \end{cases} \tag{26}$$

where $j = 1, 2, \cdots, J_t$. J_t and B_j^t denote the maximum number of training steps for the transmitter and the number of codewords in the jth sub-codebook, respectively. Also, we have $\Delta_j^t = \left\lceil \frac{L_t}{\prod_{u=1}^{j} B_u^t} \right\rceil$. If the module result equals to zero, the last codeword in the codebook is selected. The values of B_j^t and J_t must satisfy $\prod_{j=1}^{J_t} B_j^t = L_t$. All the B_j^t codewords will be trained at this step and the results are recorded as $\left(\zeta_1^t, \zeta_2^t, \cdots \zeta_{B_j^t}^t\right)$, where $\zeta_i^t = \left\| \mathbf{H}_{n,n} \mathbf{e}_i^t \right\|_F^2$, $i = 1, 2, \cdots, B_j^t$. Then, the optimal beamforming gain ζ_*^t is updated as follows:

$$\zeta_*^t = \max\left(\zeta_1^t, \zeta_2^t, \cdots \zeta_{B_j^t}^t, \zeta_*^t\right). \tag{27}$$

Let $l_j \in \{1, 2, \cdots, L_t\}$ be the index of the best codeword so that $\left\| \mathbf{H}_{n,n} \mathbf{c}_{l_j}^t \right\|_F^2 = \zeta_*^t$ and $\mathbf{c}_{l_j}^t$ be the referenced codeword for the $(j+1)$th iteration. As $\mathbf{e}_{B_1^t}^t = \mathbf{c}_{l_0}^t$, the original referenced codeword $\mathbf{c}_{l_0}^t$ is covered in the first sub-codebook and it is trained in the first iteration. Finally, the iteration training procedure is terminated when $\Delta_j^t = 1$ and the beamforming vector for the nth transmit subarray is set as $\widehat{\mathbf{f}}_n = \mathbf{c}_{l_{J_t}}^t$. The transmit beam training algorithm is summarized in Algorithm 1.

On the basis of transmit beam training results, the second procedure determines the combining vectors at the receiver according to the following criteria

$$\widehat{\mathbf{w}}_m = \max_{\mathbf{w}_m \in \mathbf{C}^r} \left\| \mathbf{w}_m^H \mathbf{H}_{m,m} \widehat{\mathbf{f}}_m \right\|_F^2. \tag{28}$$

The receive beam training procedure is initialized by selecting an original referenced codeword $\mathbf{c}_{l_0}^r$ from the predefined codebook $\mathbf{C}^r$ randomly, where $l_0 \in \{1, 2, \cdots, L_r\}$. The optimal beamforming gain is set as

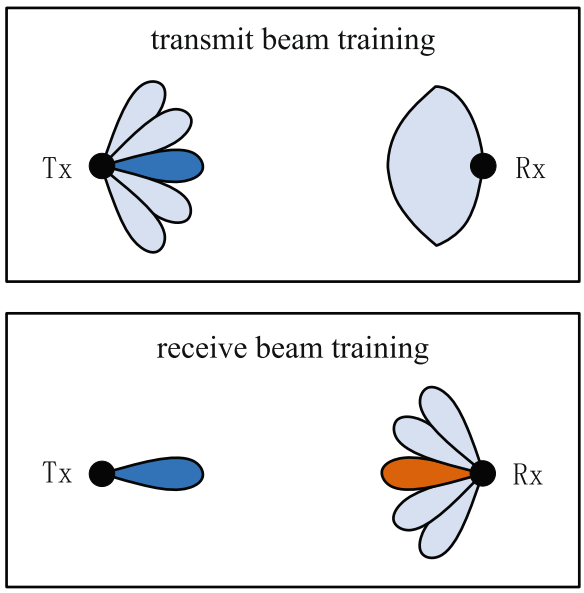

Fig. 3 Illustration of the beam training procedure

Algorithm 1 Algorithm for Beam Training at the Transmitter

1: **Input:** codebook $\mathbf{C}^t$ with size L_t generated by (10)
2: For the nth subarray at Tx, $n = 0 : N-1$
3: Select original referenced codewords $\mathbf{c}_{l_0}^t$ from $\mathbf{C}^t$ randomly, set the optimal beamforming gains as $\zeta_*^t = 0$ and initialize the iteration step as $j = 1$
4: Construct sub-codebooks $\mathbf{E}_j^t$ by (30.), train all these codewords, renew ζ_*^t by (31) and record the index of the best codewords as l_j.
5: If $\Delta_j^t = 1$, go to step 6, otherwise, set $j := j+1$, back to step 4.
6: Set the beamforming vector $\widehat{\mathbf{f}}_n = \mathbf{c}_{l_{j_t}}^t$ for the nth subarray at Tx.
7: End for
8: **Output:** the desired RF precode matrix $\mathbf{F} = diag\left(\widehat{\mathbf{f}}_0, \widehat{\mathbf{f}}_1, \cdots, \widehat{\mathbf{f}}_{N-1}\right)$.

$\zeta_*^r = 0$ at present. For the jth step, a sub-codebook $\mathbf{E}_j^r = \left[\mathbf{e}_1^r, \mathbf{e}_2^r, \cdots, \mathbf{e}_{B_j^r}^r\right]$ is generated as follow, if $j = 1$,

$$\mathbf{e}_i^r = \mathbf{c}^r_{\bmod\left(l_{j-1}+i\Delta_j^r, L_r\right)}, i = 1, 2, \cdots, B_j^r \tag{29}$$

else

$$\mathbf{e}_i^r = \begin{cases} \mathbf{c}^r_{\bmod\left(l_{j-1}-i\Delta_j^r, L_r\right)} & i = 1, 2, \cdots, \left\lfloor \frac{B_j^r}{2} \right\rfloor \\ \mathbf{c}^r_{\bmod\left(l_{j-1}+\left(i-\left\lfloor \frac{B_j^r}{2} \right\rfloor\right)\Delta_j^r, L_r\right)} & i = \left\lfloor \frac{B_j^r}{2} \right\rfloor + 1, \cdots, B_j^r \end{cases} \tag{30}$$

where $j = 1, 2, \cdots, J_r$. J_r and B_j^r denote the maximum number of training steps for the receiver and the number of codewords in the jth sub-codebook, respectively. Also, we have $\Delta_j^r = \left\lfloor \frac{L_r}{\prod_{u=1}^{j} B_u^r} \right\rfloor$. If the module result equals to zero, the last codeword in the codebook is selected. The values of B_j^r and J_r must satisfy $\prod_{j=1}^{J_r} B_j^r = L_r$. All the B_j^r codewords will be trained at this step and the results are recorded as $\left(\zeta_1^r, \zeta_2^r, \cdots \zeta_{B_j^r}^r\right)$, where $\zeta_i^r = \left\| \left(\mathbf{e}_i^r\right)^H \mathbf{H}_{m,m} \mathbf{f}_m \right\|_F^2$, $i = 1, 2, \cdots, B_j^r$. Then, the optimal beamforming gain ζ_*^r is updated as follows:

$$\zeta_*^r = \max\left(\zeta_1^r, \zeta_2^r, \cdots \zeta_{B_j^r}^r, \zeta_*^r\right). \tag{31}$$

Let $l_j \in \{1, 2, \cdots, L_r\}$ be the index of the best codeword so that $\left\| \left(\mathbf{c}_{l_j}^r\right)^H \mathbf{H}_{m,m} \mathbf{f}_m \right\|_F^2 = \zeta_*^r$ and $\mathbf{c}_{l_j}^r$ be the referenced codeword for the $(j+1)$th iteration. As $\mathbf{e}_{B_1^r}^r = \mathbf{c}_{l_0}^r$, the original referenced codeword $\mathbf{c}_{l_0}^r$ is covered in the first sub-codebook and it is trained in the first iteration. Finally, the receive training procedure is terminated when $\Delta_j^r = 1$ and the beamcombining vector for the mth receive subarray is set as $\widehat{\mathbf{w}}_m = \mathbf{c}_{l_{j_r}}^r$.

Algorithm 2 Algorithm for Beam Training at the Receiver

1: **Input:** codebook $\mathbf{C}^r$ with size L_r generated by (11)
2: For the mth subarray at Rx, $m = 0 : M-1$
3: Select original referenced codewords $\mathbf{c}_{l_0}^r$ from $\mathbf{C}^r$ randomly, set the optimal beamforming gains as $\zeta_*^r = 0$, and initialize the iteration step as $j = 1$
4: Construct sub-codebooks $\mathbf{E}_j^r$ by (30), train all these codewords, renew ζ_*^r by (31) and record the index of the best codewords as l_j .
5: If $\Delta_j^r = 1$, go to step 6, otherwise, set $j := j+1$, back to step 4.
6: Set the combining vector $\widehat{\mathbf{w}}_m = \mathbf{c}_{l_{j_r}}^r$ for the mth subarray at Rx
7: End for
8: **Output:** the desired RF combine matrix $\mathbf{W} = diag\left(\widehat{\mathbf{w}}_0, \widehat{\mathbf{w}}_1, \cdots, \widehat{\mathbf{w}}_{M-1}\right)$.

For description convenience, a small size transmit codebook designed according to (10) with L_t, $B_j^t = 2$, and $J_t = 3$ is taken as an example. Figure 4 shows an ergodic tree for the proposed beam training algorithm. The algorithm is started from training the first codeword in the codebook and is finished by three iterative training steps. The codewords whose indexes are circled by dashed lines

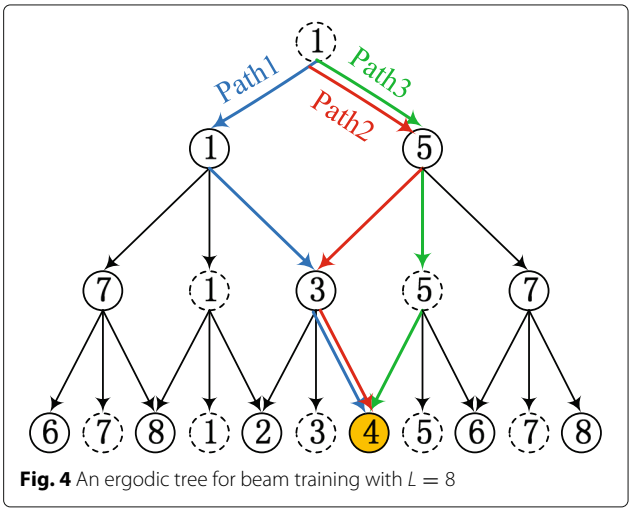

Fig. 4 An ergodic tree for beam training with $L = 8$

are selected as referenced codewords for different steps. It can be seen from the picture that more than one path exits between the first chosen codeword and the final optimized codeword. Assuming that the fourth codeword is the desired one, there are three paths achieving the destination codeword as shown in Fig. 4. If errors occur in the first or second step, they can be revised by latter steps. So, the proposed algorithm can tolerate errors in some steps and thus improve the system performance.

Assume that $L_t = L_r = L$, $J_t = J_r = J$, and $B_1^t = B_1^r = B_2^t = B_2^r = \cdots B_{J_t}^t = B_{J_r}^r = B_j$, the proposed algorithm needs $(N+M)JB_j$ times of training. For the algorithms in [25], the number of training is $\left(K_t + K_r + K^2\right)N$ for Algorithms 1 and $K_t + K_r + K^2N$ for Algorithms 2, where K_t (K_r) denotes the number of codewords trained in the initial coarse beamforming training phase for the transmitter (receiver), and K denotes the number of codewords trained in the beamforming refinement phase. Considering an exhaustive search using (23), it requires NL^2 times of training, which has a sharp increase when the codebook size becomes large.

The comparison of the number of beam training for different algorithms and some numerical examples are summarized in Table 1. For a fair treatment for different algorithms, let $L = K_tK = K_rK$. Assume that $N = M = 2$ or 4, $B_j = 2$, the maximum number of training steps is $J = 5$, so $L_t = L_r = 32$. As can be seen from Table 1, the exhaustive search required for (23) takes much more training time and energy consumption than the others. The number of training for Algorithm 1 and Algorithm 2 in [25] is linear with the root mean square of the codebook size. In contrast, the complexity of the proposed algorithm is approximately logarithmic with the codebook size. Therefore, the complexity of the proposed algorithm is close to that of Algorithm 1, 2 in [25] when the subarray size is small. However, the proposed algorithm can achieve a high beam resolution at a lower cost of training time and energy consumption than Algorithm 1, 2 in [25]. In the proposed scheme, both the transmitter and the receiver are required to allocate a certain area of memory space to keep codewords and record the results of multiple feedback. In addition, the amount of feedback is proportional to the number of iterations. Thus, the proposed scheme can improve the system performance by the sacrifice of memory space.

Table 1 Complexity comparison with different algorithms

Algorithms	Number of Training	Parameters	$N=2$	$N=4$
Equation (23)	NL^2	$L=32$	2048	4096
		$K_t=8$		
Algorithm 1 in [25]	$\left(K_t+K_r+K^2\right)N$	$K_r=8$	64	128
Algorithm 2 in [25]	$K_t+K_r+K^2N$	$K=4$	48	80
Proposed Algorithm	$(N+M)JB_j$	$B_j=2$ $J=5$	40	80

5 Simulation results

In this section, numerical results are presented to evaluate the effectiveness of the proposed design criterion with the optimal channel quality and the beam training scheme with low complexity. We consider a 45 GHz MIMO system with the subarray structure in Fig. 2 and $N = M = 4$, $N_t = N_r = 32$, thus each subarray has $P = Q = 8$ antennas. The system is optimized at $R = 100$ m, $z_0 = 0$ and $\theta = \phi = 0°$, which satisfies the optimal normalized subarray separation product $N_{ssp} = \frac{S_tS_r}{\lambda R} = \frac{1}{4}$ in (18). We set $S_t = 10S_r$ and $d_t = d_r = \lambda / 2$ as a practical placement for the antennas. SNR is set to be -5 dB in our simulations.

Figure 5 shows the relation between EDoF and normalized subarray separation product. The maximum EDoF can be achieved at many points because of the periodicity and symmetry of trigonometric functions. According to (20) and (21), $EDoF_{\min} \approx 0.99$ and $EDoF_{\max} \approx 3.81$, which agree with the two points on the curve where $N_{ssp} = 0$ and $N_{ssp} = \frac{1}{4}$, respectively. The design constraint in (18) is difficult to be met in practice. So the number of data streams N_{ss} is often set to be smaller than $EDoF_{\max}$, then the required EDoF can be set as $N_{ss} \leqslant EDoF_r \leqslant EDoF_{\max}$. For example, we have two data streams and let $EDoF_r = N_{ss} = 2$. The minimum normalized subarray separation product for $EDoF_r$ can be estimated as $\widehat{N}_{ssp} \approx 0.09$ by the use of (22) and the result is much smaller than $\frac{1}{M\cos\theta}$.

Figures 6 and 7 investigate how sensitive the performance of channel matrix is to the position shift z_0 and the orientation θ of the receiver under four different scenarios with transmission distances $R = 100$ m or 110 m and

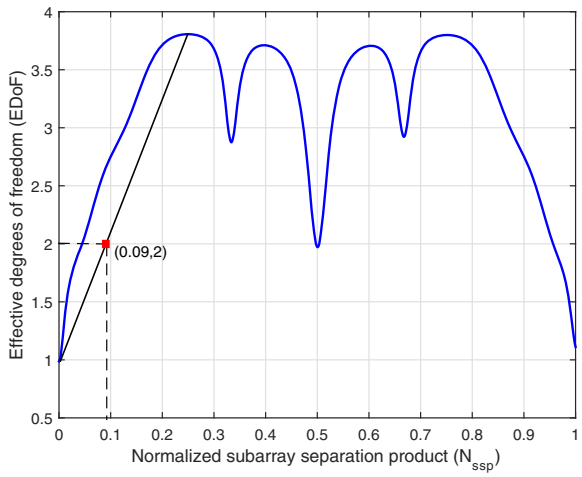

Fig. 5 EDoF versus normalized subarray separation product N_{ssp}

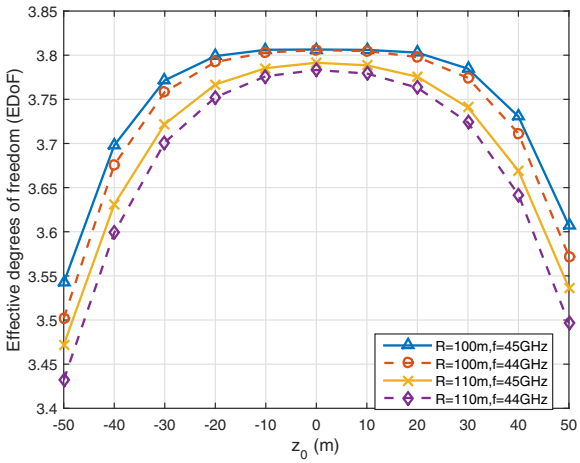

Fig. 6 EDoF versus position shift z_0

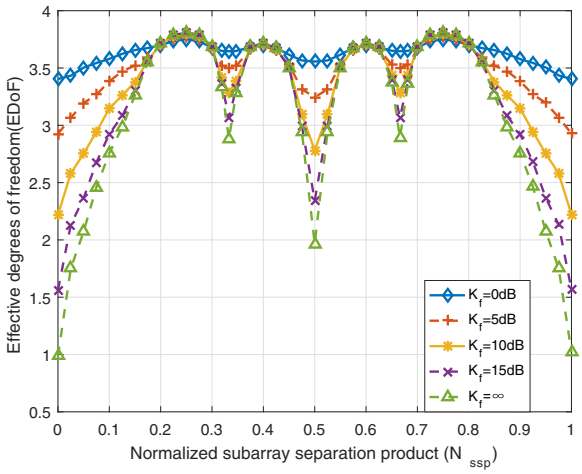

Fig. 8 EDoF versus normalized subarray separation product N_{ssp} with different K_f

carrier frequencies $f = 44$ or 45 GHz. Both Fig. 6 and Fig. 7 show that the $R = 100$ m and $f = 45$ GHz scenario has the highest EDoF and the $R = 110$ m and $f = 44$ GHz scenario has the lowest EDoF. The proposed criterion is not sensitive to the displacement and the orientation of the receive antennas. For instance, under the $R = 100$m and $f = 45$ GHz scenario, the EDoF at $z_0 = 50$ m is 5.3% lower than the maximum EDoF in Fig. 6 and the EDoF at $\theta = 45°$ is 5.8% lower than the maximum EDoF in Fig. 7. The figures also indicate that the transmission distance has higher impact on the EDoF of the system than the carrier frequency because the scenarios with $R = 100$ m achieve higher EDoF than those with $R = 110$ m.

Figure 8 illustrates the average EDoF as a function of the normalized subarray separation product by 10,000 channel realizations. It can be seen that as K_f increases the system becomes increasingly sensitive to the normalized subarray separation product. When $K_f = 0$ dB, the EDoF, and thus the system capacity, is almost independent of the normalized subarray separation product. Besides, the existence of the NLoS component gives an increase in the EDoF at those points deviating from the optimal criterion. An intuitive explanation is that the NLoS component causes the multipath effect which can increase the rank of the channel response matrix.

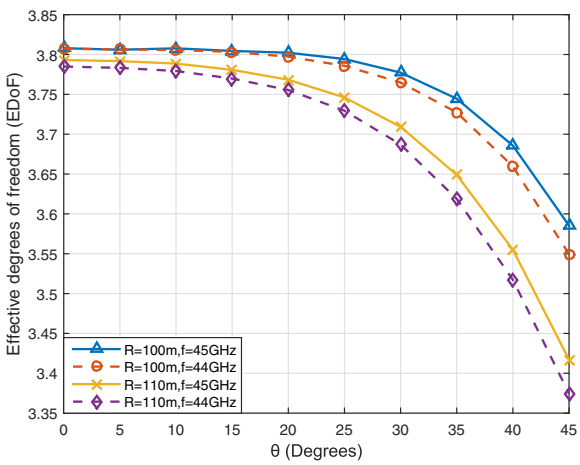

Fig. 7 EDoF versus orientation angle θ

We compare three antenna array structures with $N = M = 4$, $N_t = N_r = 32$ and $K_f = 10$ dB, i.e., (1) proposed optimally designed subarray structure with $S_t = 129.1$ cm, $S_r = 12.91$ cm and $d_t = d_r = \frac{\lambda}{2} = 0.33$ cm, (2) structure designed according to [8] with uniform antenna separations, $d_t = D_t = d_r = D_r = \sqrt{\frac{\lambda R}{32}} = 14.43$ cm, $S_t = (P-1)\,d_t + D_t = 115.47$ cm and $S_r = (Q-1)\,d_r + D_r = 115.47$ cm, (3) traditional ULA structure with $d_t = D_t = d_r = D_r = \frac{\lambda}{2} = 0.33$ cm, $S_t = (P-1)\,d_t + D_t = 2.64$ cm and $S_r = (Q-1)\,d_r + D_r = 2.64$ cm, which are summarized in Table 2. Figure 9 gives the cumulative distribution function (CDF) of capacity in randomized antenna array placements for three structures. The position shift z_0, the angles θ, ϕ, and the distance R in Fig. 2 are taken as random variables uniformly distributed in the ranges $[-10\,\text{m}, 10\,\text{m}]$, $[-90°, 90°]$, $[-90°, 90°]$ and $[90\,\text{m}, 110\,\text{m}]$, respectively. We find that the optimally designed subarray structure performs best among them

Table 2 Parameters for three antenna array structures

Structures	d_t (cm)	D_t (cm)	S_t (cm)	d_r (cm)	D_r (cm)	S_r (cm)
(1)	0.33	126.77	129.10	0.33	10.58	12.91
(2)	14.43	14.43	115.47	14.43	14.43	115.47
(3)	0.33	0.33	2.67	0.33	0.33	2.67

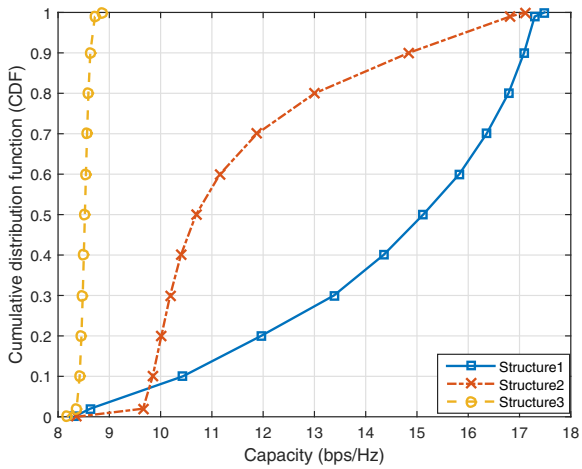

Fig. 9 Cumulative distribution function (CDF) of capacity for three antenna array structures

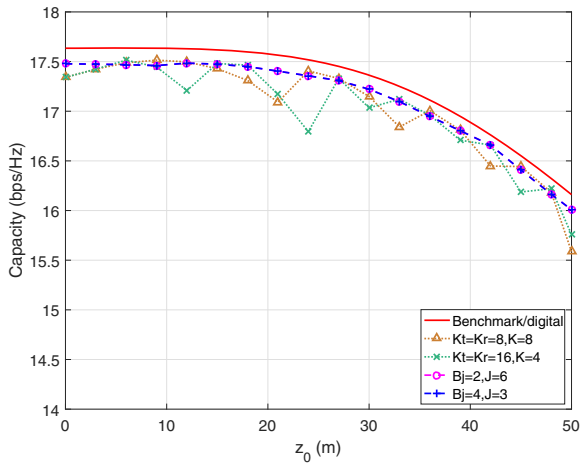

Fig. 11 Comparison between the proposed algorithm and Algorithm 2 in [25]

and the third structure is the worst due to large correlation between antennas. Although the second structure has a larger size than the optimally designed one, it still has a small performance loss due to the disadvantages of wider lobes.

Figures 10 and 11 show the capacity as a function of θ and z_0, where $L_t = L_r = L = 64$ is the same for all Tx and Rx subarrays and $R = 100$ m. The capacity obtained by the decomposition of the channel $\mathbf{H}$ into N non-interfering parallel eigenmodes in [9] is also plotted as the benchmark. In other words, the benchmark is calculated using a digital scheme. It is shown that the capacity of the proposed algorithm approaches the benchmark and is less sensitive to the angle θ than Algorithm 1, 2 in [25]. The proposed algorithm and Algorithm 1 are further compared in Fig. 11 with respect to values of B_j, J, K_t, K_r and K. To be fair, the sizes of codebook are set as $L_t = L_r = K_tK = K_rK$. On the condition that L_t and L_r keep constant, B_j and J have little impact on the performance of the proposed algorithm. In contrast, the performance of Algorithm 2 has a small fluctuation for different K_t, K_r and K combinations. Therefore, the proposed algorithm is a more stable solution.

Figure 12 shows capacity for the proposed algorithm with different codebook sizes as a function of SNR in dB. K_f is set to be 10 dB. $B_j = 2$ is the same for all Tx and Rx subarrays. In general, the capacity is improved as codebook size increases. However, the capacity gap between the benchmark and the proposed scheme becomes larger as SNR increases. When the codebook size is lager than two times of the number of antennas in each subarray, the capacity improvement is not so apparent. The more

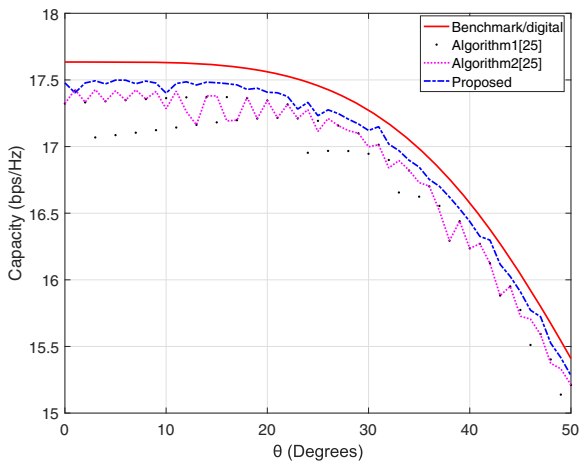

Fig. 10 Comparison between different algorithms with $B_j = 2, J = 6, K_t = K_r = K = 8$

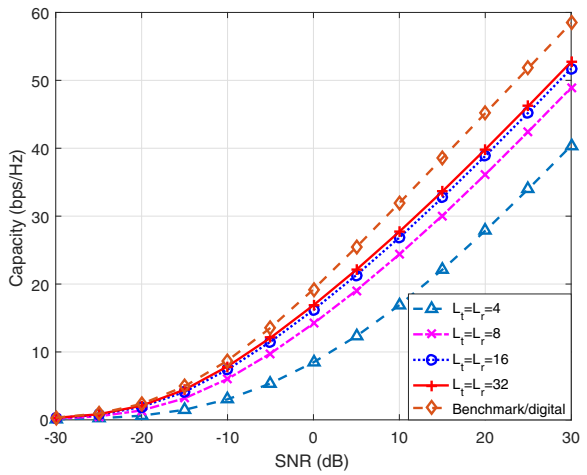

Fig. 12 Capacity as a function of SNR with different codebook sizes

codewords the codebook has, the more training time and energy consumption are required. Particularly, it is a compromise practice to set the codebook size to be two times of the number of antennas in each subarray.

The convergence rate of the proposed algorithm for different receive positions is presented in Fig. 13. The proposed algorithm is started from training the codeword with index $l_0 = 1$. The receiver with the least position shift z_0 converges to the maximum capacity quickly as the original referenced codeword is close to the desired one. The initial values of these curves decrease as the receiver position shift increases. However, all the curves converge to the same capacity when the sixth iterative training step is completed. Besides, the convergence rate of the proposed algorithm depends on the channel condition, the number of antennas in each subarray, the codebook size, and the choice of the original referenced codeword.

6 Conclusions

The subarray structure was designed to realize high EDoF MIMO transmission for wireless channels with a strong LoS component. The criterion showed that the optimal subarray separation product is proportional to the transmission distance multiplied by the wavelength and inversely proportional to the number of RF chains multiplied by the cosine of the spherical angle θ at the receiver. The iterative training scheme had the complexity logarithmic with the codebook size and outperformed some existing algorithms. Although LoS channels are in general rank deficient, the communication system with the proposed scheme can afford both array gains and spatial multiplexing gains through carefully designed antenna subarray spacing and appropriate beam training at both the transmitter and the receiver. In addition, the system designed based on the optimal criterion is robust to the geometrical change and the misplacement in practice. And the beam training scheme has the ability to tolerate some abrupt errors occurred in earlier training steps. Therefore, it is feasible to create high rank MIMO systems over LoS channels by special geometrical configurations and effective beamforming schemes. Finally, more research on flexible styles of the antenna deployment such as uniform plan arrays (UPAs) are expected in the future work.

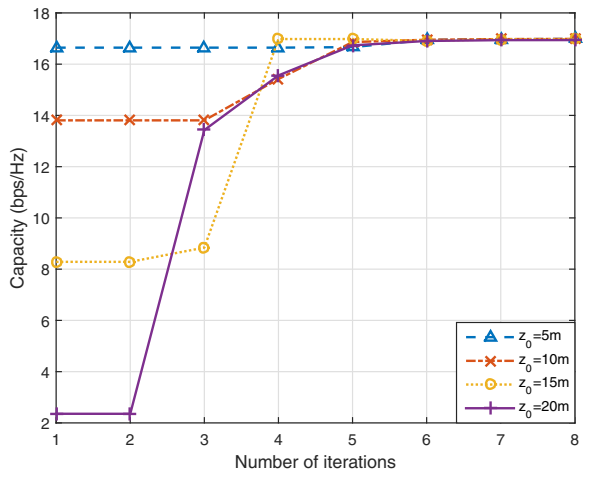

Fig. 13 The convergency tendency of the proposed algorithm with $L = 256$, $B_j = 2$, $J = 8$

Endnote

[1] A codebook based beam training scheme to determine $\mathbf{f}_n$ and $\mathbf{w}_m$ will be explained in more details in Section 4.

Acknowledgments
This work was supported by National Natural Science Foundation of China under Grants 61471120 and 61422105, Key Laboratory of Cognitive Radio and Information Processing Ministry of Education (Guilin University of Electronic Technology) under Grants CRKL160203.

Competing interests
The authors declare that they have no competing interests.

Author details
[1]School of Information Science and Engineering, Southeast University, Nanjing 210096, China. [2]The Key Laboratory of Cognitive Radio and Information Processing, Ministry of Education, Guilin University of Electronic Technology, Guilin 541004, China. [3]Institute for Digital Communications, University of Erlangen, Cauerstrasse 7, D-91058 Erlangen, Germany.

Received: 6 July 2016 Accepted: 1 February 2017
Published online: 14 February 2017

References

1. Z Pi, J Choi, R Heath, Millimeter-wave gigabit broadband evolution toward 5g: fixed access and backhaul. IEEE Commun. Mag. **54**(4), 138–144 (2016)
2. Z Pi, F Khan, An introduction to millimeter-wave mobile broadband systems. Commun. Mag. IEEE. **49**(6), 101–107 (2011)
3. B Gaucher, B Floyd, S Reynolds, U Pfeiffer, J Grzyb, A Joseph, E Mina, B Orner, H Ding, R Wachnik, et al, Silicon germanium based millimetre-wave ics for gbps wireless communications and radar systems. Semiconductor Sci. Technol. **22**(1), 236 (2006)
4. D Gesbert, M Shafi, D-S Shiu, PJ Smith, A Naguib, From theory to practice: an overview of mimo space-time coded wireless systems. Selected Areas Commun. IEEE J. **21**(3), 281–302 (2003)
5. TS Rappaport, GR Maccartney, MK Samimi, S Sun, Wideband millimeter-wave propagation measurements and channel models for future wireless communication system design. Commun. IEEE Trans. **63**(9), 3029–3056 (2015)
6. MR Akdeniz, Y Liu, MK Samimi, S Sun, S Rangan, TS Rappaport, E Erkip, Millimeter wave channel modeling and cellular capacity evaluation. Selected Areas Commun. IEEE J. **32**(6), 1164–1179 (2014)
7. L Zhou, Y Ohashi, in *Wireless Communications and Networking Conference (WCNC), 2014 IEEE*. Low complexity millimeter-wave los-mimo precoding systems for uniform circular arrays (IEEE, Istanbul, 2014), pp. 1293–1297
8. F Bohagen, P Orten, GE Oien, in *Wireless Communications and Networking Conference, 2005 IEEE*. Construction and capacity analysis of high-rank line-of-sight mimo channels, vol. 1 (IEEE, New Orleans, 2005), pp. 432–437
9. E Torkildson, U Madhow, M Rodwell, Indoor millimeter wave mimo: feasibility and performance. Wireless Commun. IEEE Trans. **10**(12), 4150–4160 (2011)
10. D Gesbert, H Bölcskei, DA Gore, AJ Paulraj, Outdoor mimo wireless channels: models and performance prediction. Commun. IEEE Trans. **50**(12), 1926–1934 (2002)
11. C-X Wang, F Haider, X Gao, X-H You, Y Yang, D Yuan, H Aggoune, H Haas, S Fletcher, E Hepsaydir, Cellular architecture and key technologies for 5g wireless communication networks. Commun. Mag. IEEE. **52**(2), 122–130 (2014)

12. SK Yong, C-C Chong, An overview of multigigabit wireless through millimeter wave technology: potentials and technical challenges. EURASIP J. Wireless Commun. Netw. **2007**(1), 1–10 (2006)
13. J He, T Kim, H Ghauch, K Liu, G Wang, in *Globecom Workshops (GC Wkshps), 2014*. Millimeter wave mimo channel tracking systems (IEEE, Austin, 2014), pp. 416–421
14. O El Ayach, S Rajagopal, S Abu-Surra, Z Pi, RW Heath, Spatially sparse precoding in millimeter wave mimo systems. Wireless Commun. IEEE Trans. **13**(3), 1499–1513 (2014)
15. S Sun, TS Rappaport, RW Heath, A Nix, S Rangan, Mimo for millimeter wave wireless communications: beamforming, spatial multiplexing, or both? IEEE Commun. Mag. **52**(12), 110–121 (2014)
16. Y Wu, R Schober, DWK Ng, C Xiao, G Caire, Secure massive MIMO transmission with an active eavesdropper. IEEE Trans. Inf. Theory. **62**, 3880–3900 (2016)
17. W Roh, JY Seol, J Park, B Lee, J Lee, Y Kim, J Cho, K Cheun, F Aryanfar, Millimeter-wave beamforming as an enabling technology for 5g cellular communications: theoretical feasibility and prototype results. IEEE Commun. Mag. **52**(2), 106–113 (2014)
18. A Alkhateeb, OE Ayach, G Leus, RWH Jr, Channel estimation and hybrid precoding for millimeter wave cellular systems. IEEE J. Selected Topics Signal Process. **8**(5), 831–846 (2014)
19. S Han, I Chih-Lin, Z Xu, C Rowell, Large-scale antenna systems with hybrid analog and digital beamforming for millimeter wave 5g. IEEE Commun. Mag. **53**(1), 186–194 (2015)
20. J Wang, Z Lan, CS Sum, CW Pyo, J Gao, T Baykas, A Rahman, R Funada, F Kojima, I Lakkis, in *IEEE Vehicular Technology Conference Fall*. Beamforming codebook design and performance evaluation for 60 ghz wideband wpans, (Anchorage, 2009), pp. 1–6
21. J Wang, Z Lan, CW Pyo, T Baykas, CS Sum, MA Rahman, R Funada, F Kojima, I Lakkis, H Harada, Beam codebook based beamforming protocol for multi-gbps millimeter-wave wpan systems. IEEE J. Selected Areas Commun. **27**(8), 1–6 (2009)
22. S Buzzi, C D'Andrea, On clustered statistical mimo millimeter wave channel simulation (2016). Online, arXiv:1604.00648v2, [cs.IT]
23. E Ben-Dor, TS Rappaport, Y Qiao, SJ Lauffenburger, in *Global Telecommunications Conference (GLOBECOM 2011), 2011 IEEE*. Millimeter-wave 60 ghz outdoor and vehicle aoa propagation measurements using a broadband channel sounder, (Houston, 2011), pp. 1–6
24. AM Sayeed, V Raghavan, Maximizing mimo capacity in sparse multipath with reconfigurable antenna arrays. IEEE J. Selected Topics Signal Process. **1**(1), 1561–66 (2007)
25. L Zhou, Y Ohashi, in *Vehicular Technology Conference (VTC Fall), 2015 IEEE 82nd*. Fast codebook-based beamforming training for mmwave mimo systems with subarray structures (IEEE, 2015), pp. 1–5